Coseismic slip distribution of the 2002 M_W7.9 Denali fault earthquake, Alaska, determined from GPS measurements

Sigrún Hreinsdóttir,[1] Jeffrey T. Freymueller,[1] Hilary J. Fletcher,[1] Christopher F. Larsen,[1] and Roland Bürgmann[2]

Received 31 March 2003; revised 9 May 2003; accepted 16 May 2003; published 1 July 2003.

[1] On 3 November 2002 an M_W7.9 earthquake occurred in central Alaska. The earthquake ruptured portions of the Susitna Glacier, Denali, and Totschunda faults. Inversion of the GPS-measured displacement field indicates that the event was dominated by a complex, right-lateral strike-slip rupture along the Denali fault. GPS sites closest to the epicenter show the effect of thrust motion on the Susitna Glacier fault. The preferred coseismic slip model, with M_W7.8, indicates relatively low slip on the western part of the rupture and high slip from about 60 km east of the hypocenter extending to the junction of the Denali and Totschunda faults. We find mostly shallow slip from the surface to 15 km depth, but the inversion suggests one large deep slip patch about 110 km east of the hypocenter. Our model predicts surface slip in good agreement with surface geological observations, where model resolution is good. *INDEX TERMS:* 1242 Geodesy and Gravity: Seismic deformations (7205); 1243 Space geodetic surveys; 7209 Seismology: Earthquake dynamics and mechanics; 8107 Tectonophysics: Continental neotectonics; 8158 Plate motions—present and recent (3040). **Citation:** Hreinsdóttir, S., J. T. Freymueller, H. J. Fletcher, C. F. Larsen, and R. Bürgmann, Coseismic slip distribution of the 2002 M_W7.9 Denali fault earthquake, Alaska, determined from GPS measurements, *Geophys. Res. Lett.*, *30*(13), 1670, doi:10.1029/2003GL017447, 2003.

1. Introduction

[2] On 3 November 2002, an M_W7.9 earthquake occurred on the Denali fault, central Alaska. The earthquake was preceded by an M_W6.7 right-lateral strike-slip earthquake on 23 October, with its epicenter only 22 km west of the M_W7.9 epicenter [*Eberhart-Phillips et al.*, 2003]. These earthquakes are the largest earthquakes to occur on the Denali fault in recorded history. The 2002 Denali fault earthquake ruptured the surface for about 340 km along three major faults. It first ruptured 40 km along the Susitna Glacier fault, a thrust fault south of and splaying off of the Denali fault. Then it ruptured for 220 km along the Denali fault, with nearly pure right lateral slip, to the junction of the Denali and Totschunda faults where it stepped over to the Totschunda fault and ruptured another 80 km [*Eberhart-Phillips et al.*, 2003].

[3] Many existing GPS points in Alaska were surveyed following the M_W7.9 earthquake. Here we present coseismic displacements for the M_W7.9 Denali fault earthquake for sites measured within one week of the earthquake and permanent GPS sites in Alaska. We invert these GPS data to determine the coseismic slip distribution of the earthquake.

2. GPS Data and Analysis

[4] We use data from 40 GPS sites in this study (Figure 1, Table S1[1]); 28 campaign GPS sites from the interior of Alaska (21), south central Alaska (5), and the Yukon (2) (triangles) and 12 permanent GPS sites in the interior and south central Alaska (black squares). To limit the impact of postseismic deformation on the coseismic displacements we mostly used data from sites that were surveyed within one week of the M_W7.9 earthquake. To increase spatial coverage of site distribution for the inversion we included data from a few far-field sites measured about 10 days after the earthquake. We selected two sites in the Yukon that were closest to the rupture south-east of the fault, and sites in south central Alaska that had at least two days of post earthquake measurements and antennas centered and leveled at pickup.

[5] All the sites used here had multiple years of measurements prior to the earthquake, and most had precise velocities [*Fletcher*, 2002; *Zweck et al.*, 2002]. Twelve of these sites were surveyed following the 23 October M_W6.7 earthquake, all within 80 km of its epicenter. Other sites were last surveyed from 2 months to 2 years prior to the earthquake. In addition to these measurements, 12 permanent GPS sites were operating within 500 km of the epicenter.

[6] We analyzed the GPS data using the GIPSY/OASIS II software (release 5) developed at the Jet Propulsion Laboratory (JPL) using the JPL non-fiducial orbits. Data from each day were processed separately to obtain loosely constrained daily network solutions. The daily GPS solutions were then transformed into the International Terrestrial Reference Frame 1997 (ITRF97) [*Boucher et al.*, 1999] using about 15 global reference sites (variable day to day) to define the 7 parameter Helmert transformation [*Freymueller et al.*, 2000].

[7] We used two different methods to estimate displacements due to the earthquake. For permanent sites and sites measured following the M_W6.7 earthquake we averaged the four days prior to and four days following the earthquake and estimated displacements from these merged solutions.

[1]Geophysical Institute, University of Alaska Fairbanks, Fairbanks, Alaska, USA.
[2]Department of Earth and Planetary Science, University of California Berkeley, Berkeley, California, USA.

0094-8276/03/2003GL017447$05.00

[1] Supporting material is available via Web browser or via Anonymous FTP from ftp://ftp.agu.org, directory "apend" (Username = "anonymous", Password = "guest"); subdirectories in the ftp site are arranged by paper number. Information on searching and submitting electronic supplements is found a http://www.agu.org/pubs/esupp_about.html.

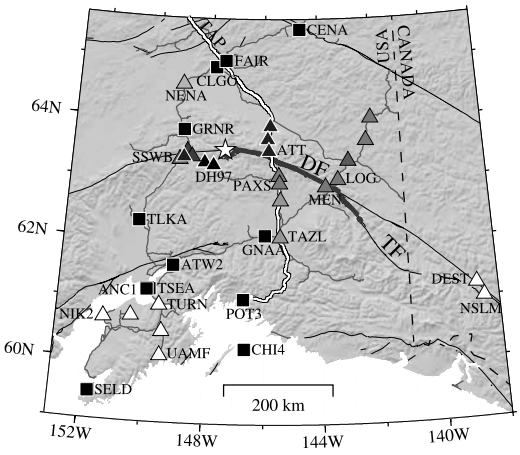

Figure 1. GPS sites used in this study. Triangles show campaign GPS sites and squares show permanent GPS sites. Black sites were measured within a day of the earthquake, white sites were measured more than a week after the earthquake. Shades of gray show intermediate times. The epicenter of the M_W7.9 Denali fault earthquake is shown with a white star and its surface rupture is shown with the thick gray line [*Eberhart-Phillips et al.*, 2003]. Black lines indicate major faults in Alaska, gray lines show roads, and the Trans-Alaska oil pipeline (TAP) is shown with a white line. Names of selected sites are shown. Note that 6 GPS sites are located between DH97 and SSWB, W and SW of the epicenter. DF-Denali fault, TF-Totschunda fault.

For other sites we fit a line plus offset to the station time series. We only used the first 3 days of post-earthquake measurements at each site to limit postseismic signal in the data. The uncertainties in the displacements were scaled based on the scatter in the measurements, considering each component independently.

[8] The GPS data show a right lateral deformation field (Figure 2 and Figure S1[1]). North of the fault, sites show eastward motion and sites to the south show westward motion, relative to ITRF97. The largest measured horizontal displacement of 3.107 ± 0.004 m was at a site (MEN) just south of the main strand of the Denali fault, near where the maximum surface offset was measured in the eastern part of the rupture [*Eberhart-Phillips et al.*, 2003]. Observed vertical displacements were generally smaller than the horizontal, indicating mostly strike slip motion (Figure S2[1]). With a few exceptions, sites north of the fault moved up and sites south of the fault moved down. Only 6 sites had more than 5 cm of measured vertical displacement and all but one had less than 10 cm. The maximum subsidence of 0.246 ± 0.007 m was measured at MEN. Sites southwest of the epicenter have a more northerly coseismic displacement than expected for pure strike slip motion, supporting seismic and geological data that indicate thrusting along the Susitna Glacier fault [*Eberhart-Phillips et al.*, 2003].

3. Inversion for Fault Slip Model

[9] We used a 9 plane geometric approximation to the surface rupture of the Denali and Totschunda faults for the inversion of the GPS data (Table S2[1]). The model was extended to the west, using the mapped Denali fault trace, in order to span both the aftershock region for the M_W6.7 and M_W7.9 earthquakes and thus test for re-rupture of the M_W6.7 segment. Each plane was split into 3 km × 3 km tiles extending down to 18 km depth with a dip of 90° in accord with teleseismic body wave analysis [*Kikuchi and Yamanaka*, 2002]. We applied Laplacian smoothing between the tiles, with a zero slip boundary condition below 18 km depth. For the Susitna Glacier thrust fault we added 8 tiles with a strike of 81°. For the lower 4 tiles, intersecting the Denali fault at about 8 km depth, a dip of 48° was assumed based on the focal mechanism from the local network [*Eberhart-Phillips et al.*, 2003]. The upper 4 tiles, intersecting the surface at the mapped surface rupture, were fixed to 25° dip to match field observations [*Eberhart-Phillips et al.*, 2003], with Laplacian smoothing between the tiles.

[10] We used a bounded variable least squares (BVLS) inversion [*Stark and Parker*, 1995] to estimate coseismic slip on each model fault tile, allowing only right lateral slip on the Denali and Totschunda faults and only thrust motion on the Susitna Glacier fault (both assumptions are consistent

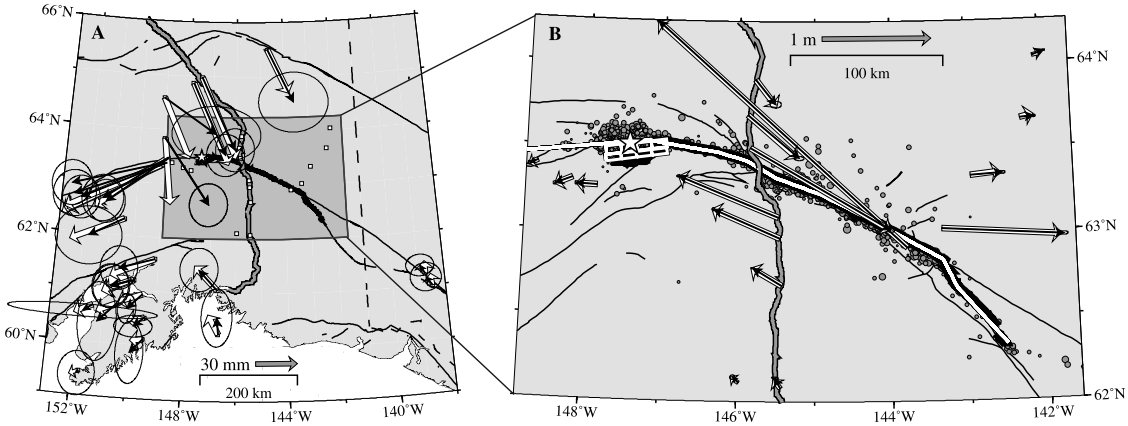

Figure 2. Coseismic displacements (black) from the M_W7.9 earthquake with 95% confidence ellipses and inversion results (white), for far-field (A) and near-field (B) sites. The white star shows the M_W7.9 epicenter, circles show relocated aftershocks [*Ratchkovski et al.*, 2003], thick line indicates earthquake rupture [*Eberhart-Phillips et al.*, 2003]. The white line (B) shows the model fault used in this study. Displacements are shown at two different scales in the two panels.

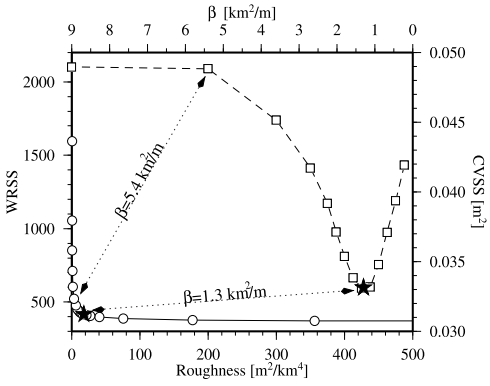

Figure 3. Trade-off curve between roughness and misfit (circles and solid line) and the CVSS as function of smoothing factor (squares with dashed line). Dotted lines connect two models with the same smoothing factor. We exclude the three sites with the largest coseismic displacement in estimating the CVSS. The stars show the preferred model, with smoothing of $\beta = 1.3$ km^2/m.

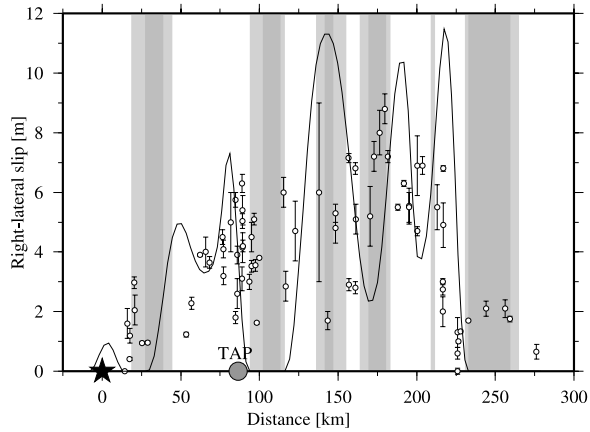

Figure 5. Estimated right lateral surface offset of the prefered model (line) compared to geological surface measurements from *Eberhart-Phillips et al.* [2003]. By inverting synthetic data of uniform slip we identified areas of poor model resolution along the surface, with dark gray areas showing <50% resolved and light gray <70%.

with seismic results). We computed the Green's functions, **G**, relating slip on each fault tile, s_i, to displacement at a GPS site, $\vec{d}_j$, assuming an elastic half space and a Poisson's ratio of 0.25 [*Okada*, 1985]. For the inversion we used displacements relative to the southernmost station in the network, SELD. We used 117 data to estimate 770 model parameters, so an additional constraint such as smoothing is required to make the inversion stable. We measured roughness using the Laplacian operator, **L**, weighted roughness using a smoothing factor β, and minimized the (unitless) weighted residual sum of squares (WRSS) and the roughness of the model:

$$\underbrace{||\mathbf{W}(\mathbf{G}\vec{s} - \vec{d})||^2}_{misfit} + \beta^2 \underbrace{||\mathbf{L}\vec{s}||^2}_{roughness} \quad (1)$$

($\mathbf{W}^T\mathbf{W} = \mathbf{\Sigma}^{-1}$ where $\mathbf{\Sigma}$ is the GPS data covariance matrix.)

[11] Changing β changes the importance assigned to data fit and smoothness, and produces a family of models with varying misfit and roughness (Figure 3). We want to select a smoothing factor for which the solution fits the data well, but is not excessively rough. Selecting the smoothing factor based only on a tradeoff curve can be highly subjective, so we also used the Cross-Validation Sum of Squares (CVSS) to determine the most reasonable smoothing factor [*Matthews and Segall*, 1993; *Freymueller et al.*, 1994]. The CVSS is a measure of the model's ability to predict observations. Each station in turn in taken out of the data set and its displacement predicted based on a model fit to the other data. The CVSS is the sum of squares of the predicted residuals. In this case, the three stations with the largest coseismic displacements (MEN, LOG, and ATT) turned out not to be predictable by the other stations and had prediction residuals 1–2 orders of magnitude larger than the sum of squares for all other sites. We therefore decided to use the CVSS test without these three sites. This gives a minimum CVSS for $\beta \sim 1.3$ km^2/m which also gives a reasonable roughness versus misfit tradeoff (stars in Figure 3). The three sites excluded in the CVSS analysis are located in very sensitive locations for the inversion.

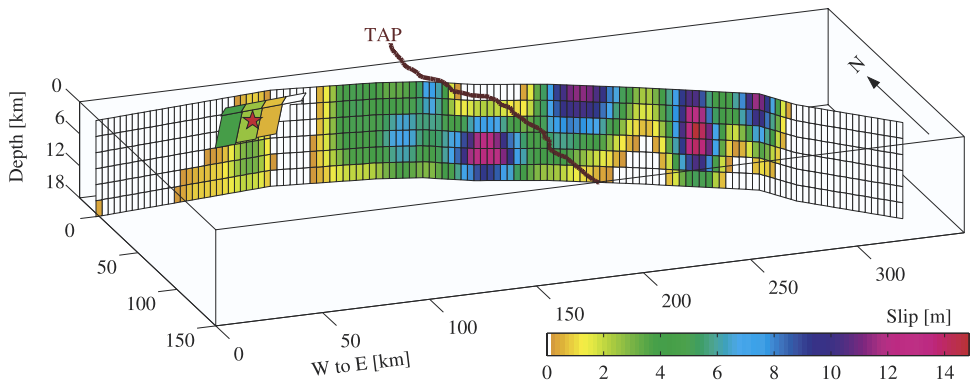

Figure 4. Coseismic slip distribution for the M_W7.9 Denali fault earthquake for the preferred model. The model has up to 15 m of right lateral slip along the Denali fault and up to 4 m of thrusting on the Susitna Glacier fault. Most slip is found above 12–15 km depth, but we find a deep slip patch just east of where the pipeline (TAP) crosses the fault. The star indicates the hypocenter of the M_W7.9 earthquake, located at the Sustina Glacier thrust fault.

MEN and LOG are closest to where the maximum geological offset was measured and are relatively isolated from other sites (40 km from the next site). ATT is located where geological observations indicate a gradient in the surface offset. This indicates that we might benefit from the use of spatially variable smoothing, but for this paper we restrict ourselves to a constant smoothing factor. The preferred coseismic slip model is shown in Figure 4. The corresponding predicted coseismic displacements are shown in Figure 2 (white vectors).

4. Discussion and Conclusions

[12] The modeled slip distribution varies considerably from west to east along the Denali fault. Relatively low slip is estimated for the westernmost 60 km of the rupture but further east, to the junction of the Denali and Totschunda faults, high slip is resolved. Little to no slip is found on the Totschunda fault but up to four meters of thrust motion is estimated on the Susitna Glacier fault. The total moment release of the preferred model is 5.8×10^{20} Nm (M_W7.8), slightly lower than estimated from teleseismic data [*Eberhart-Phillips et al.*, 2003].

[13] The modeled surface slip shows a similar pattern to the measured surface offsets, varying from little to no dextral offset in the epicentral region to about 10 m of slip just west of the Denali-Totschunda fault junction (Figure 5). The surface slip observations were not used in the inversion, so they provide an independent test of the model. Although there are slight offsets between the locations of peak slip in the two data sets, the overall agreement is good. The average 2 m of thrust motion on the Susitna Glacier fault, corresponding to an M_W7.0 subevent, is also consistent with surface observations but has a slightly lower seismic moment than estimated from teleseismic data [*Eberhart-Phillips et al.*, 2003].

[14] Surface measurements resolve dextral offsets of up to 2 m along the Totschunda fault but in the preferred model very little slip is found on the fault. The Totschunda fault is not well covered by the coseismic GPS data and tests with inverting synthetic data of uniform slip at given depth indicate that model resolution for shallow slip on the fault is very poor. Resolution for slip from 6–12 km depth is good, so the lack of slip in the model may indicate that coseismic slip on the Totschunda fault was shallow.

[15] No slip is estimated west of the epicenter where the M_W6.7 earthquake ruptured the Denali fault prior to the M_W7.9 earthquake. Tests with synthetic data show that this part of the model is well resolved, so the lack of model slip shows that the M_W7.9 earthquake did not re-rupture the M_W6.7 rupture zone. Very little slip is found on the Denali fault near the hypocenter, although model resolution here is not as good as to the west. About 2–4 m of deep slip is found below the thrust fault which might indicate rupture of both faults, or might be the result of a trade off between slip on the Susitna Glacier fault and the Denali fault.

[16] In general, slip on the fault extends from the surface to 10–15 km depth. However, the model has a patch of very deep slip just east of the pipeline crossing, corresponding to an M_W7.4 subevent. All relocated aftershocks are less than 10 km deep and do not give any indication of deep slip [*Ratchkovski et al.*, 2003]. We have done several tests, removing stations from the inversion, adding potential splay faults to the model, and allowing dip slip motion along the fault, but we find a similar deep slip patch in all inversions. These tests indicate that this result is probably real and reflects some local complication. The deep slip is found in a complex area where there are many splay faults both north and south of the Denali fault [*Plafker et al.*, 1994]. Aftershocks are spread over a broad area and the largest aftershock of the Denali fault earthquake, *M*5.8 on 3 November, occurred in this region (no focal mechanism is available for this aftershock, as it occurred within the coda of the M_W7.9 event) [*Ratchkovski et al.*, 2003].

[17] The GPS coseismic displacements from the M_W7.9 earthquake agree with right lateral strike slip motion along the Denali and Totschunda faults and thrust motion on the Susitna Glacier fault. The earthquake did not re-rupture the M_W6.7 rupture zone. Variations in coseismic slip along the fault and with depth reflect the complex nature of the earthquake. Our results are in good agreement to surface offsets and seismic measurements.

[18] **Acknowledgments.** Data from the Yukon were provided by P. Flück and M. Schmidt at the Geological Survey of Canada. We are grateful to E. Calais, J. Elliot, J. Greenberg, L. Hennig, M. Jadamec, B. Johns, J. Kalbas, B. MacCormack, D. Moudry, E. Price, K. Ridgway, F. Rolandone, N. Rozell, J. Sklar, J. Stachnik, D. Templeton, and T. Tin for fieldwork assistance. We thank N. Ratchkovski for discussions on aftershock locations. The manuscript benefited from helpful reviews and suggestions from N. King and an anonymous reviewer. This research was supported by NSF grant EAR-0328043 to J. Freymueller and R. Hansen, by the Alaska Earthquake Information Center, and by the UAF Geophysical Institute.

References

Boucher, C., Z. Altamimi, and P. Sillard, The 1997 International Terrestrial Reference Frame (ITRF97), *IERS Tech. Note 27*, Int. Earth Rotation Serv., Paris, 1999.

Eberhart-Phillips, D., P. J. Haeussler, and J. T. Freymueller, et al., The 2002 Denali fault earthquake, Alaska: A large magnitude, slip-partitioned event, *Science*, *300*, 1113–1118, 2003.

Fletcher, H. J., Tectonics of interior Alaska from GPS measurements, Ph.D. thesis, 257 pp., Univ. Alaska Fairbanks, Fairbanks, Alaska, 2002.

Freymueller, T. J., S. C. Cohen, and H. J. Fletcher, Spatial variations in present-day deformation, Kenai Peninsula, Alaska, and their implications, *J. Geophys. Res*, *105*(B4), 8079–8102, 2000.

Freymueller, J. T., N. E. King, and P. Segall, The co-seismic slip distribution of the Landers earthquake, *Bull. Seis. Soc. Amer.*, *84*(3), 649–659, 1994.

Kikuchi, M., and Y. Yamanaka, Source rupture processes of the central Alaska earthquake of Nov. 3, 2002, inferred from teleseismic body waves (+the 10/23 M6.7 event), EIC seismological note - No. 129, Earthquake Research Institute (ERI), Univ. Tokyo, Tokyo, 2002.

Matthews, M., and P. Segall, Statistical inversion of crustal deformation data and estimation of the depth distribution of slip in the 1906 earthquake, *J. Geophys. Res.*, *98*(B7), 12,153–12,163, 1993.

Okada, Y., Surface deformation due to shear and tensile faults in a half-space, *Bull. Seis. Soc. Amer.*, *75*(4), 1135–1154, 1985.

Plafker, G., L. Gilpin, and J. Lahr, Neotectonic map of Alaska, Map in *The Geology of North America, Decade of North American Geology*, vol. G-1, edited by G. Plafker and H. C. Berg, Geol. Soc. Amer., Boulder, Colorado, 1994.

Ratchkovski, N. A., R. A. Hansen, and J. C. Stachnik, The 7.9 Denali fault earthquake of November 3, 2002: Aftershock locations, moment tensors, and focal mechanisms from the regional and temporary seismic network data, *Seis. Res. Lett.*, *74*(2), SSA 2003 Annual Meeting, 236, 2003.

Stark, P. B., and R. L. Parker, Bounded-variable least-squares: An algorithm and application, *Comput. Stat.*, *10*(2), 129–141, 1995.

Zweck, C., J. T. Freymueller, and S. C. Cohen, Three-dimensional elastic dislocation modeling of the postseismic response to the 1964 Alaska earthquake, *J. Geophys. Res.*, *107*(B4), doi:10.1029/2001JB000409, 2002.

S. Hreinsdóttir, Geophysical Institute, University of Alaska Fairbanks, 903 Koyukuk Dr, Fairbanks, AK 99775, USA. (sigrun@giseis.alaska.edu)